



Communication

# Synthesis and Characterization of Cationic Tetramethyl Tantalum(V) Complex

Raju Dey <sup>1,2</sup> , Janet C. Mohandas <sup>1</sup>, Manoj K. Samantaray <sup>1</sup>, Ali Hamieh <sup>1</sup>, Santosh Kavitate <sup>1</sup>, Yin Chen <sup>1,3</sup>, Edy Abou-Hamad <sup>1</sup>, Luigi Cavallo <sup>1</sup>, Albert Poater <sup>4,\*</sup>  and Jean-Marie Basset <sup>1,\*</sup>

<sup>1</sup> King Abdullah University of Science & Technology, KAUST Catalysis Center (KCC), Thuwal 23955-6900, Saudi Arabia; rajudey@nitc.ac.in (R.D.); janet.mohandas@kaust.edu.sa (J.C.M.); manoj.samantaray@kaust.edu.sa (M.K.S.); ali.hamieh@kaust.edu.sa (A.H.); santosh.kavitate@kaust.edu.sa (S.K.); chenying@iccas.ac.cn (Y.C.); edy.abouhamad@kaust.edu.sa (E.A.-H.); luigi.cavallo@kaust.edu.sa (L.C.)

<sup>2</sup> Department of Chemistry, National Institute of Technology Calicut, NIT Campus, Kozhikode 673 601, India

<sup>3</sup> College of Chemistry & Chemical Engineering, Central South University, Changsha 410083, China

<sup>4</sup> Institut de Química Computacional i Catàlisi and Departament de Química, Universitat de Girona, c/ M<sup>a</sup> Aurèlia Capmany 69, 17003 Girona, Catalonia, Spain

\* Correspondence: albert.poater@udg.edu (A.P.); jeanmarie.basset@kaust.edu.sa (J.-M.B.); Tel.: +34-972-419403 (A.P.)

Received: 1 October 2018; Accepted: 28 October 2018; Published: 1 November 2018



**Abstract:** A novel method for the synthesis of the homogeneous homoleptic cationic tantalum(V)tetramethyl complex  $[(TaMe_4)^+ MeB(C_6F_5)_3]^-$  from neutral tantalumpentamethyl ( $TaMe_5$ ) has been described, by direct demethylation using  $B(C_6F_5)_3$  reagent. The aforesaid higher valent cationic tantalum complex was characterized precisely by liquid state  $^1H$ -NMR,  $^{13}C$ -NMR, and  $^1H$ - $^{13}C$ -NMR correlation spectroscopy.

**Keywords:** tantalum; cationic; tungsten; DFT calculations; homoleptic; reaction mechanism; boron

## 1. Introduction

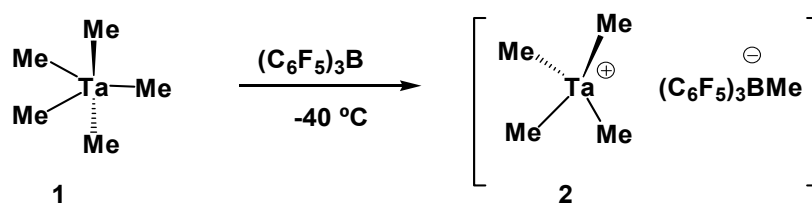
Tantalum alkyl complexes are of vital importance in current organometallic chemistry, from the point of view of stoichiometric reactions and mainly in catalysis [1–4]. Since 1974, tantalumpentamethyl ( $TaMe_5$ , **1**) has the honour to be the simplest homoleptic complex of this class of compounds [5,6]. **1** was discovered by Richard Schrock and the structure was not unravelled until 1992 by Albright [7] and Haaland et al. [8].  $TaMe_5$  is rather unstable thermally and, consequently, **1** is highly prone to autocatalytically degradation [6]. Recently, in our previous communication [9], we checked that grafting this unstable  $TaMe_5$  complex to the silica surface by a Surface Organometallic Chemistry (SOMC) strategy enhances its thermal stability due to the formation of the stable grafted  $(\equiv Si-O-)TaMe_4$ . The latter complex proved to be a nice precursor for alkane metathesis, leading to the formation of a surface monopodal tantalum methylidene dimethyl catalyst [9,10].

With the precedents of Buchmeiser and co-workers who developed the first cationic tungsten-oxo-alkylidene-NHC complex (NHC = *N*-heterocyclic carbene) [11,12], where the NHC was introduced to stabilize the cationic metal centre, together with the also tungsten based cationic complex  $WMe_5^+$  [13], to improve the catalysts in terms of reactivity and selectivity, and taking into account the idea of increasing the electrophilicity on metal centre, we deepened into the idea of generating the cationic species of  $TaMe_5$ . This change planned to enter the field of predictive catalysis. Unfortunately, the drawback for tantalum with respect to tungsten is that the similar cationic Ta-complexes are scarce in literature [14–16], whereas there are several examples with stable cationic

tantalum complexes containing one or more nitrogen [17], phosphorous [18] and cyclopentadienyl containing ligands [19–21].

## 2. Results

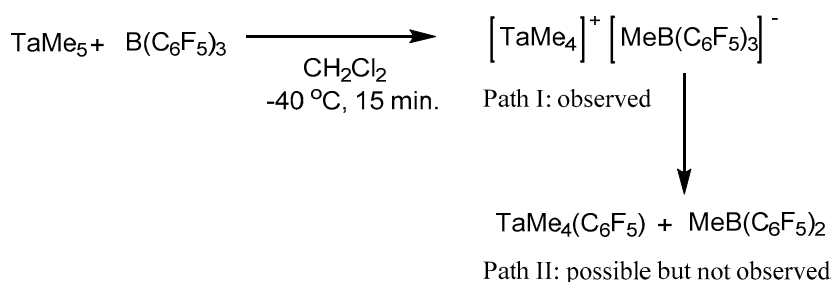
As a part of our continuing research program to explore any novel application of tantalumpentamethyl complex, we report here a method for the synthesis of the homogeneous cationic  $[\text{TaMe}_4]^+$  together with  $[\text{MeB}(\text{C}_6\text{F}_5)_3]^-$  anion (2), starting from the neutral  $\text{TaMe}_5$ . The experimental procedure was straightforward: The simple mixture of bulky and non-coordinating boron Lewis acid,  $\text{B}(\text{C}_6\text{F}_5)_3$ , with 1, at low temperature ( $-40\text{ }^\circ\text{C}$ ) generates the cationic complex 2 (see Scheme 1), since above this temperature the undesired phenomenon of degradation appears in a rather facile way.



**Scheme 1.** Demethylation of homoleptic  $\text{TaMe}_5$  complexes by strong electrophilic  $\text{B}(\text{C}_6\text{F}_5)_3$ .

Preliminarily, we tried the synthesis of  $\text{TaMe}_4^+$  using an organic Lewis acid, tris(pentafluorophenyl)boron. The latter species is known to form a non-nucleophilic anion after demethylation reaction, a strategy that it is valid also with titanium [22,23], zirconium [24], or hafnium [24–26]. When the reaction was monitored by nuclear magnetic resonance (NMR) spectroscopy, at  $-40\text{ }^\circ\text{C}$ , the peak corresponding to  $\text{TaMe}_5$  at 0.9 ppm in  $^1\text{H}$ -NMR (Figure 1a) almost completely disappeared in less than 15 min due to the fast reaction between  $\text{TaMe}_5$  and  $\text{B}(\text{C}_6\text{F}_5)_3$ , and two new peaks at 2.6 ppm and 0.5 ppm appeared (Figure 1b) [27].

Based on the above observations one can assume two possibilities (Scheme 2); path I consists of simple demethylation by the  $\text{B}(\text{C}_6\text{F}_5)_3$  from  $\text{TaMe}_5$  leading to the formation of cationic tantalum complex; whereas in path II there would be a chance for the formation of a neutral tantalum complex by simple ligand exchange. Path II could take place in a one-step mechanism from the original  $\text{TaMe}_5$ , however it seems more plausible after path I.



**Scheme 2.** Possible reaction between  $\text{TaMe}_5$  and  $\text{B}(\text{C}_6\text{F}_5)_3$ .

Looking in detail at the  $^1\text{H}$ -NMR chemical shift at +0.5 ppm, it is confirmed that it corresponds to  $[\text{Me-B}(\text{C}_6\text{F}_5)_3]^-$ , in agreement with past studies [13,25,26]. The peak at 2.6 ppm corresponded to the cationic tantalum complex  $[\text{TaMe}_4]^+$ , upfield with respect to the signal at 0.9 ppm assigned to the resonance for the methyl proton of  $\text{TaMe}_5$ .

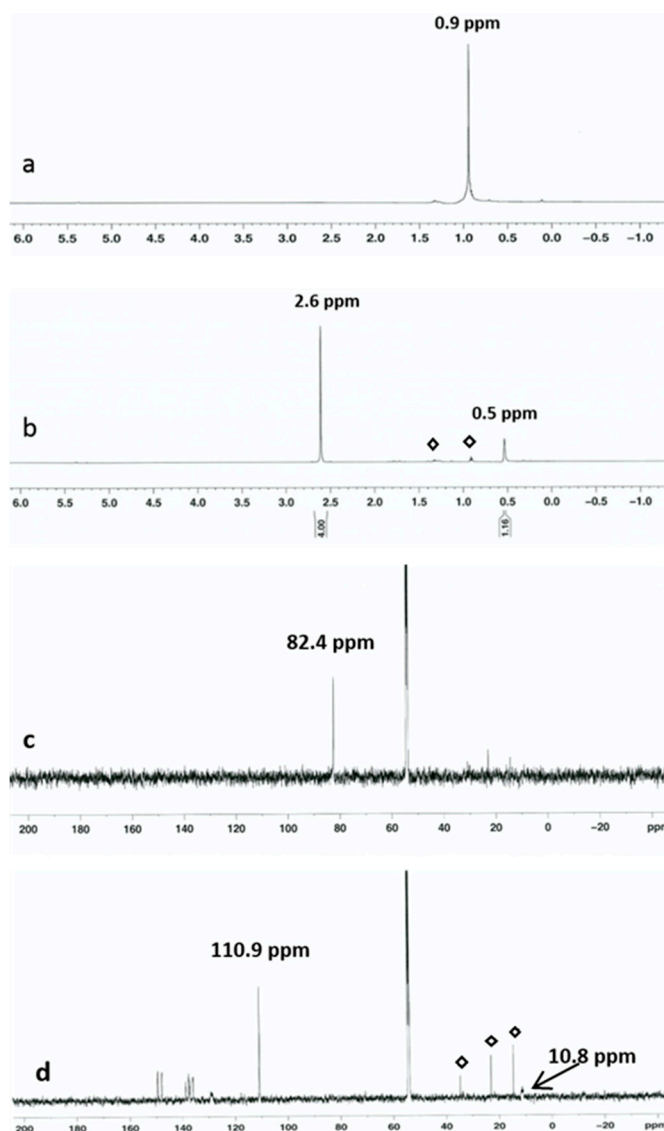


**Figure 1.** (a)  $^1\text{H}$ -NMR spectra of  $\text{TaMe}_5$ ; (b)  $^1\text{H}$ -NMR spectra of  $[\text{TaMe}_4]^+[\text{MeB}(\text{C}_6\text{F}_5)_3]^-$ ; (c)  $^{13}\text{C}$ -NMR spectrum of  $\text{TaMe}_5$ ; (d)  $^{13}\text{C}$ -NMR spectrum of  $[\text{TaMe}_4]^+[\text{MeB}(\text{C}_6\text{F}_5)_3]^-$ , (at  $-40^\circ\text{C}$ , peak marked by ( $\diamond$ ) is due to the slight amounts of pentane vapor which was used as a coolant during the low temperature reaction in the glovebox).

Switching to  $^{13}\text{C}$ -NMR, the spectrum also clearly showed that the peak corresponding to  $\text{TaMe}_5$  at 82.4 ppm (Figure 1c) was completely replaced by two peaks at 110.9 ppm  $[\text{TaMe}_4]^+$  and 10.8 ppm (Figure 1d) corresponding to the  $[\text{Me-B}(\text{C}_6\text{F}_5)_3]^-$  anion which is in good agreement with the literature value reported for the  $[\text{Me-B}(\text{C}_6\text{F}_5)_3]^-$  anion [26]. We also found in the  $^1\text{H}$ - $^{13}\text{C}$  correlation spectra that the peak at 0.5 ppm in  $^1\text{H}$ -NMR correlates with the peak at 10.8 ppm in  $^{13}\text{C}$ -NMR and the peak at 2.6 ppm in  $^1\text{H}$ -NMR correlated with the peak at 110.9 ppm in  $^{13}\text{C}$ -NMR (Supplementary Materials Figure S1). In separate experiments we synthesised  $^{13}\text{C}$  labelled  $\text{Ta}(^{13}\text{CH}_3)_5$  and upon treatment with  $\text{B}(\text{C}_6\text{F}_5)_3$  in dichloromethane solution, we identified incorporation of the labelled methyl in  $[(^{13}\text{CH}_3)\text{B}(\text{C}_6\text{F}_5)_3]^-$  anion in the final product. The above experiment clearly indicates that in  $[\text{MeB}(\text{C}_6\text{F}_5)_3]^-$ , 'Me' came from  $\text{TaMe}_5$ . These spectroscopic data strongly support the formation of cationic complex 2 and is in favour of path I. The ionic product generated by the reaction was fairly stable at temperatures below  $-40^\circ\text{C}$  and in the absence of light. However, upon warming a dichloromethane solution of 2 from  $-40^\circ\text{C}$  to  $0^\circ\text{C}$ , a very fast decomposition of the cationic complex was observed with the release of gaseous methane.

Density Functional Theory (DFT) calculations (M06/Def2TZVPP(smd)//PBE0-d3bj/SVP [28], at temperature = 298.15 °C and pressure = 1354 atm [29–31] to remove the overestimation of the entropy [32–34]) were envisaged to unravel the mechanistic insights of the first demethylation of TaMe<sub>5</sub>. The energy barrier to overcome was found to be 6.8 kcal/mol (Figure 2a), releasing 15.4 kcal/mol (see Table 1), thus the favourable kinetic and thermodynamic character of the reaction, respectively, confirmed the observed experimental facile demethylation. Furthermore, the energy barrier for this reaction was even 2.3 kcal/mol lower with respect to the recent homologous process studied for WMe<sub>6</sub>, together with a release of 1.6 kcal/mol more energy as well, confirms the experimental more facile demethylation by Ta than W based complexes [13]. It is worth pointing out that for TaMe<sub>5</sub>, the radical demethylation was not in competition with the anion demethylation, because TaMe<sub>4</sub>·radical was located 44.1 kcal/mol over TaMe<sub>5</sub>, and thus enormously disfavoured by 25.3 kcal/mol with respect to the homologous WMe<sub>5</sub>. Surprisingly, TaMe<sub>5</sub> is able to allocate easily a sixth anion like chloride, with an energy stabilization of 5.8 kcal/mol, compared with the destabilisation by 3.6 kcal/mol for WMe<sub>6</sub>, due to steric hindrance in the metal centre of the WMe<sub>6</sub>Cl<sup>−</sup> anion.

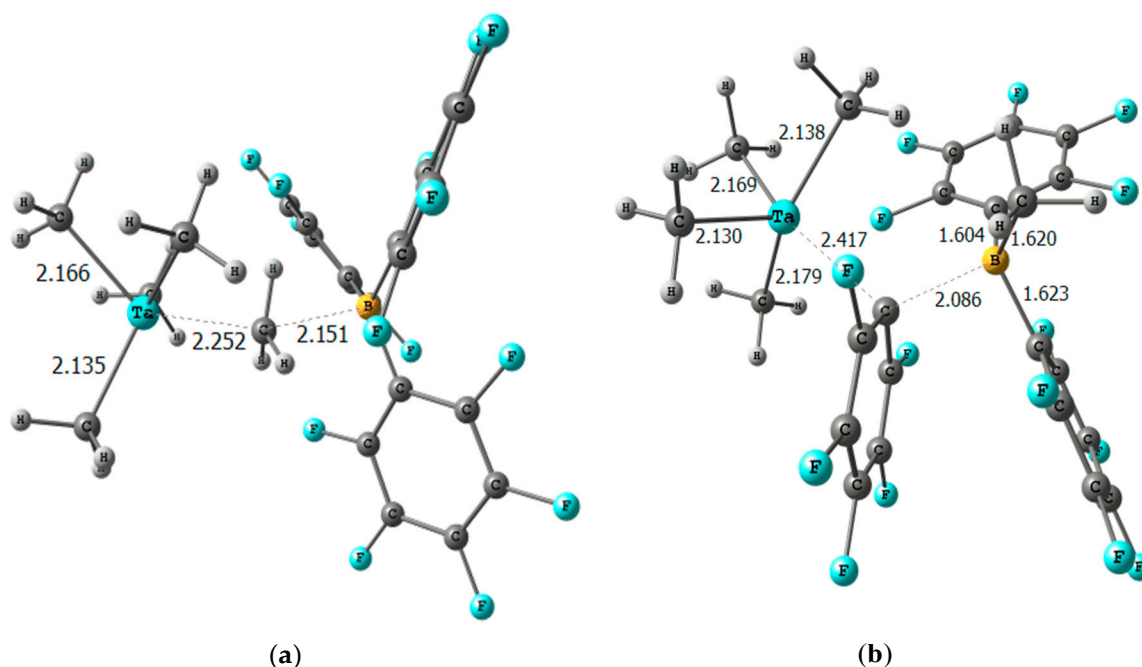


**Figure 2.** Transition states for (a) the demethylation of TaMe<sub>5</sub> by B(C<sub>6</sub>F<sub>5</sub>)<sub>3</sub> and (b) (C<sub>6</sub>F<sub>5</sub>)<sup>−</sup> transfer from B(Me)(C<sub>6</sub>F<sub>5</sub>)<sub>3</sub><sup>−</sup> to TaMe<sub>4</sub><sup>+</sup>, main distances are shown in Å.

**Table 1.** Gibbs energy values (in kcal/mol) for (a) the energy barrier of the transition state of the anion demethylation in the reaction [MMe<sub>x</sub> → MMe<sub>(x−1)</sub><sup>+</sup> + Me<sup>−</sup>], (b) the relative stability of the next demethylated anion MMe<sub>(x−1)</sub><sup>+</sup>, (c) the intermediate MMe<sub>(x−1)</sub>· after the loose of a radical methyl and (d) the addition of a chloride anion that leads to MMe<sub>x</sub>Cl<sup>−</sup> (M = Ta or W).

Catalyst	(a)	(b)	(c)	(d)
TaMe <sub>5</sub>	6.8	−15.4	44.1	−5.8
WMe <sub>6</sub>	9.1	−13.8	18.8	3.6

Here, steric effects play a key role, and the more sterically crowded W centre provides less space for a seventh coordination around the metal centre, and at the same time facilitates the loose of a methyl ligand. To evaluate the steric hindrance around the metal, SambVca steric maps were used [35–37]. The %Vbur was 74.5% for TaMe<sub>5</sub> and 79.9% for WMe<sub>6</sub>. It is worth pointing out that the quadrants for the latter hexamethylated complex were not equally occupied (see Figure 3), ranging from 75.8% to

84.0%, with 76.1% and 83.8% in between. Anyway, none of the quadrants was less occupied than the equally distributed TaMe<sub>5</sub> ones [38].

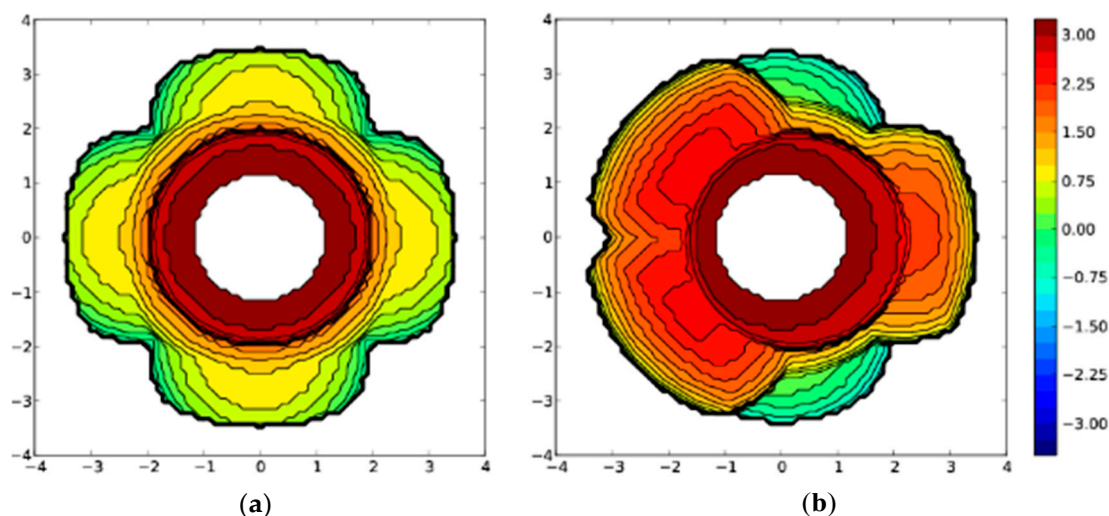


**Figure 3.** Topographic steric maps (xy plane) of the metal centres of (a) TaMe<sub>5</sub> and (b) WMe<sub>6</sub>. The corresponding metal is at the origin and one methyl of TaMe<sub>5</sub> is on the z axis. The isocontour curves of the steric maps are given in Å.

On the other hand, the substitution of a methyl ligand by a perfluorobenzene ligand from B(C<sub>6</sub>F<sub>5</sub>)<sub>3</sub>, i.e., path II in Scheme 2, requires to overcome an energy barrier that is placed at 26.8 kcal/mol with respect to TaMe<sub>5</sub>. However, from [MeB(C<sub>6</sub>F<sub>5</sub>)<sub>3</sub>]<sup>−</sup> an unaffordable energy barrier of 41.9 kcal/mol must be overcome (see Figure 2b). The overall reaction pathway following paths I and II in Scheme 2 is displayed in Figure 4. Consequently, the huge kinetic cost of path II confirms that once TaMe<sub>5</sub> is demethylated, the next cation intermediate TaMe<sub>4</sub><sup>+</sup> cannot recover an anionic ligand, i.e., (C<sub>6</sub>F<sub>5</sub>)<sup>−</sup>, from [MeB(C<sub>6</sub>F<sub>5</sub>)<sub>3</sub>]<sup>−</sup>, even though the next intermediate TaMe<sub>4</sub>(C<sub>6</sub>F<sub>5</sub>) is 11.8 kcal/mol lower in energy than TaMe<sub>5</sub>.

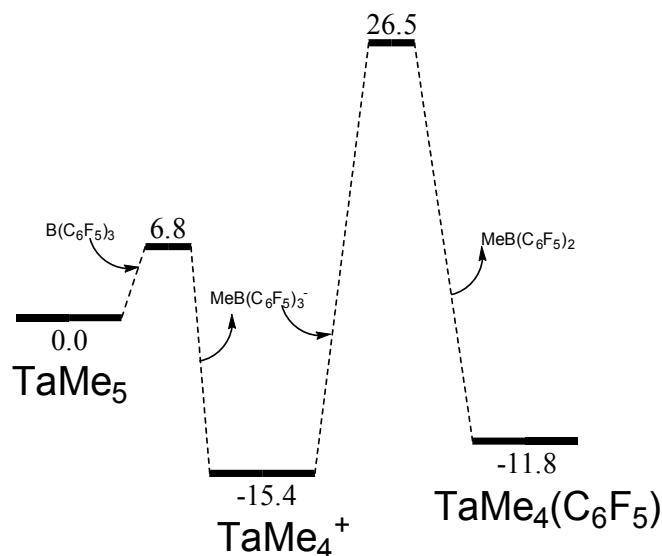


**Figure 4.** Reaction pathway for the demethylation of TaMe<sub>5</sub> with B(C<sub>6</sub>F<sub>5</sub>)<sub>3</sub> and next C<sub>6</sub>F<sub>5</sub> anionic transfer (Gibbs energies in kcal/mol referred to TaMe<sub>5</sub>).

Switching to the grafted system  $(\equiv\text{Si-O})\text{TaMe}_4$ , the demethylation process requires to overcome an energy barrier of 9.8 kcal/mol (see Figure 5 for the corresponding transition state) and the next intermediate is 5.1 kcal/mol lower in energy than the initial supported catalyst. Here the difference with tungsten is significant, because apart from facing a more facile barrier by 4.8 kcal/mol, the relative stability of the next intermediate excludes the reversibility of the demethylation observed only for W. Overall, kinetically and thermodynamically, the demethylation process is more prone with Ta based systems. Consequently, we then prepared the surface complex of  $\text{TaMe}_5$  after grafting on to the dehydroxylated Aerosil  $\text{SiO}_{2(700)}$  (Figure S2). Synthesized  $(\equiv\text{Si-O})\text{TaMe}_4$  was treated with  $\text{B}(\text{C}_6\text{F}_5)_3$  in order to get a cationic tantalum-methyl complex anchored on the surface of silica,  $[(\equiv\text{Si-O})\text{TaMe}_3]^+$ . However, after several attempts (varying reaction temperature, reaction time and solvents) we were unable to identify any well-defined heterogeneous cationic tantalum methyl complex [13], except for a mixture of decomposed tantalum methyl complex with a  $^{13}\text{C}$ -NMR signal corresponding to the formation of the anionic  $[\text{MeB}(\text{C}_6\text{F}_5)_3]^-$  (see Figures S3 and S4), indicating a probable formation of surface cationic species. The surface cationic complex decomposed much more rapidly, and it was difficult to characterize it by solid state NMR. This may be due to the unstable nature of  $8 e^- [(\equiv\text{Si-O})\text{TaMe}_3]^+$  complex.

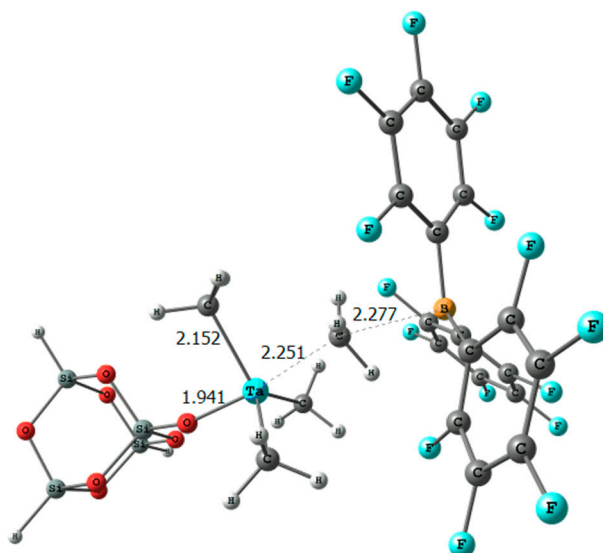


**Figure 5.** Transition state for the demethylation by  $\text{B}(\text{C}_6\text{F}_5)_3$  of  $(\equiv\text{Si-O})\text{TaMe}_4$ , main distances are shown in Å.

### 3. Conclusions

In summary, the cationic homoleptic tantalum (V)-methyl complex has been synthesized via a straightforward strategy to address the will to get a more electrophilic metal centre, generating the first tantalum-based species with such a property. The delicate equilibrium between stability and degradation was enforced to work at low temperature, and the high oxidation state cationic tantalum complex **2** was defined by liquid  $^1\text{H}$ -NMR,  $^{13}\text{C}$ -NMR and  $^1\text{H}$ - $^{13}\text{C}$  correlation spectroscopy; together with DFT calculations. Ongoing experimental studies are being undertaken in order to understand the null activity in alkane metathesis of the grafted tantalum system and will be disclosed in due time.



**Supplementary Materials:** The following are available online at <http://www.mdpi.com/2073-4344/8/11/507/s1>, Figure S1: (a) Two-dimensional (2D) liquid-state  $^1\text{H}$ - $^{13}\text{C}$  heteronuclear single quantum correlation (HSQC) NMR spectrum of  $[\text{TaMe}_4^+ \text{MeB}(\text{C}_6\text{F}_5)_3^-]$  in  $\text{CD}_2\text{Cl}_2$  recorded at  $-40^\circ\text{C}$ ; Figure S2: (a) One-dimensional (1D)  $^1\text{H}$  MAS NMR spectrum of  $(\equiv\text{Si-O})\text{TaMe}_4$  acquired at 600 MHz with a 22 kHz MAS frequency, a repetition delay of 5 s, and 8 scans. (b)  $^{13}\text{C}$  CP MAS NMR spectrum of  $(\equiv\text{Si-O})\text{TaMe}_4$  (acquired at 400 MHz) with a 10 kHz MAS frequency, 10,000 scans, a 4-s repetition delay, and a 2-ms contact time. Exponential line broadening of 80 Hz was applied prior to Fourier transformation.  $^{13}\text{C}$  CP MAS spectra were acquired at natural abundance; Figure S3. (c) One-dimensional (1D)  $^{13}\text{C}$  CP MAS NMR spectrum of  $[(\equiv\text{Si-O})\text{TaMe}_4]$  (acquired at 400 MHz) with a 10 kHz MAS frequency, (d)  $^{13}\text{C}$  CP MAS spectra of  $[(\equiv\text{Si-O})\text{TaMe}_4]$  when decomposed on the surface at room temperature during the prolonged NMR measurement.  $^{13}\text{C}$  CP MAS spectra were acquired at natural abundance; Figure S4. (e) One-dimensional (1D)  $^1\text{H}$  MAS NMR spectrum of  $[(\equiv\text{Si-O})\text{TaMe}_3^+ \text{B}(\text{C}_6\text{F}_5)_3\text{Me}^-]$  acquired at 400 MHz with a 22 kHz MAS frequency, a repetition delay of 5 s, and 8 scans; (f)  $^{13}\text{C}$  CP MAS NMR spectrum of  $[(\equiv\text{Si-O})\text{TaMe}_3^+ \text{B}(\text{C}_6\text{F}_5)_3\text{Me}^-]$ .

**Author Contributions:** Conceptualization, R.D., A.P., and J.-M.B.; experiments, R.D., J.C.M., M.K.S., A.H., S.K., Y.C., E.A.-H.; calculations, L.C. and A.P.; writing R.D., A.P., L.C. and J.-M.B.

**Funding:** This work was supported by funds from King Abdullah University of Science and Technology (KAUST) office of sponsored research (OSR). R.D. thanks National Institute of Technology, Calicut for financial support. A.P. thanks the Spanish MINECO for a project CTQ2014-59832-JIN.

**Acknowledgments:** The authors acknowledge the KAUST Nuclear Magnetic Resonance Core Lab and the technical assistance of Xianrong Guo.

**Conflicts of Interest:** The authors declare no competing financial interests.

## References and Notes

- Schrock, R.R. Alkylidene Complexes of Niobium and Tantalum. *Acc. Chem. Res.* **1979**, *12*, 98–104. [[CrossRef](#)]
- Schrock, R.R. First Isolable Transition Metal Methylene Complex and Analogs. Characterization, Mode of Decomposition, and some Simple Reactions. *J. Am. Chem. Soc.* **1975**, *97*, 6577–6578. [[CrossRef](#)]
- Roux, E.L.; Chabanas, M.; Baudouin, A.; de-Mallmann, A.; Copéret, C.; Quadrelli, E.A.; Thivolle-Cazat, J.; Basset, J.-M.; Lukens, W.; Lesage, A.; et al. Detailed Structural Investigation of the Grafting of  $[\text{Ta}(\text{=CH}t\text{Bu})(\text{CH}_2t\text{Bu})_3]$  and  $[\text{Cp}^*\text{TaMe}_4]$  on Silica Partially Dehydroxylated at  $700^\circ\text{C}$  and the Activity of the Grafted Complexes toward Alkane Metathesis. *J. Am. Chem. Soc.* **2004**, *126*, 13391–13399. [[CrossRef](#)] [[PubMed](#)]
- Freundlich, J.S.; Schrock, R.R.; Davis, W.M. Alkyl and Alkylidene Complexes of Tantalum That Contain a Triethylsilyl-Substituted Triamido–Amine Ligand. *Organometallics* **1996**, *15*, 2777–2783. [[CrossRef](#)]
- Schrock, R.R.; Meakin, P. Pentamethyl Complexes of Niobium and Tantalum. *J. Am. Chem. Soc.* **1974**, *96*, 5288–5290. [[CrossRef](#)]
- Schrock, R.R. Preparation and Characterization of  $\text{M}(\text{CH}_3)_5$  ( $\text{M} = \text{Nb}$  or  $\text{Ta}$ ) and  $\text{Ta}(\text{CH}_2\text{C}_6\text{H}_5)_5$  and Evidence for Decomposition by  $\alpha$ -Hydrogen Atom Abstraction. *J. Organomet. Chem.* **1976**, *122*, 209–225. [[CrossRef](#)]
- Albright, T.A.; Tang, H. The Structure of Pentamethyltantalum. *Angew. Chem. Int. Ed.* **1992**, *31*, 1462–1464. [[CrossRef](#)]
- Pulham, C.; Haaland, A.; Hammel, A.; Rypdal, K.; Verne, H.P.; Volden, H.V. Perfluorotriethylamine: An Amine with Unusual Structure and Reactivity. *Angew. Chem. Int. Ed.* **1992**, *31*, 1464–1467.
- Chen, Y.; Abou-hamad, E.; Hamieh, A.; Hamzaoui, B.; Emsley, L.; Basset, J.-M. Alkane Metathesis with the Tantalum Methylidene  $[(\equiv\text{SiO})\text{Ta}(\text{=CH}_2)\text{Me}_2]/[(\equiv\text{SiO})_2\text{Ta}(\text{=CH}_2)\text{Me}]$  Generated from Well-Defined Surface Organometallic Complex  $[(\equiv\text{SiO})\text{Ta}^V\text{Me}_4]$ . *J. Am. Chem. Soc.* **2015**, *137*, 588–591. [[CrossRef](#)] [[PubMed](#)]
- Chen, Y.; Ould-Chikh, S.; Abou-Hamad, E.; Callens, E.; Mohandas, J.C.; Khalid, S.; Basset, J.-M. Facile and Efficient Synthesis of the Surface Tantalum Hydride  $(\equiv\text{SiO})_2\text{Ta}^{\text{III}}\text{H}$  and Tris-Siloxy Tantalum  $(\equiv\text{SiO})_3\text{Ta}^{\text{III}}$  Starting from Novel Tantalum Surface Species  $(\equiv\text{SiO})\text{TaMe}_4$  and  $(\equiv\text{SiO})_2\text{TaMe}_3$ . *Organometallics* **2014**, *33*, 1205–1211. [[CrossRef](#)]
- Schowner, R.; Frey, W.; Buchmeiser, M.R. Cationic Tungsten-Oxo-Alkylidene-N-Heterocyclic Carbene Complexes: Highly Active Olefin Metathesis Catalysts. *J. Am. Chem. Soc.* **2015**, *137*, 6188–6191. [[CrossRef](#)] [[PubMed](#)]

12. Pucino, M.; Mougél, V.; Schowner, R.; Fedorov, A.; Buchmeiser, M.R.; Copéret, C. Cationic Silica-Supported N-Heterocyclic Carbene Tungsten Oxo Alkylidene Sites: Highly Active and Stable Catalysts for Olefin Metathesis. *Angew. Chem. Int. Ed.* **2016**, *55*, 4300–4302. [[CrossRef](#)] [[PubMed](#)]
13. Dey, R.; Samantaray, M.K.; Poater, A.; Hamieh, A.; Kavitate, S.; Abou-Hamad, E.; Callens, E.; Emwas, A.-H.; Cavallo, L.; Basset, J.-M. Synthesis and Characterization of a Homogeneous and Silica Supported Homoleptic Cationic Tungsten(VI) Methyl Complex: Application in Olefin Metathesis. *Chem. Commun.* **2016**, *52*, 11270–11273. [[CrossRef](#)] [[PubMed](#)]
14. Sanchez-Nieves, J.; Royo, P.; Mosquera, M.E.G. Synthesis of the Cation Complex  $[\text{TaCp}^*\text{Me}_3]^+$  and a Comparison of Its Reactivity with That of  $[\text{TaCp}^*\text{Me}_4]$ . *Organometallics* **2006**, *25*, 2331–2336. [[CrossRef](#)]
15. Sanchez-Nieves, J.; Royo, P. Synthesis of Neutral and Cationic Monocyclopentadienyl Tantalum Alkoxo Complexes and Polymerization of Methyl Methacrylate. *Organometallics* **2007**, *26*, 2880–2884. [[CrossRef](#)]
16. Mariott, W.R.; Gustafson, L.O.; Chen, E.Y.-X. Activation of Tantalocene(V) Alkyl and Alkylidene Complexes with Strong Organo Lewis Acids and Application to Polymerization Catalysis. *Organometallics* **2006**, *25*, 3721–3729. [[CrossRef](#)]
17. Fryzuk, M.D.; Johnson, S.A.; Rettig, S.J. Synthesis and Structure of the Tantalum Trimethyl Complex  $[\text{P}_2\text{N}_2]\text{TaMe}_3$  and Its Conversion to the Tantalum Methylidene Species  $[\text{P}_2\text{N}_2]\text{TaCH}_2(\text{Me})$  ( $[\text{P}_2\text{N}_2] = \text{PhP}(\text{CH}_2\text{SiMe}_2\text{NSiMe}_2\text{CH}_2)_2\text{PPh}$ ). *Organometallics* **1999**, *18*, 4059–4067. [[CrossRef](#)]
18. Guérin, F.; Stephan, D.W. Synthesis and Structure of the Dicationic Bisborate Adduct. *Angew. Chem. Int. Ed.* **2000**, *39*, 1298–1300. [[CrossRef](#)]
19. Anderson, L.L.; Schmidt, J.A.R.; Arnold, J.; Bergman, R.G. Neutral and Cationic Alkyl Tantalum Imido Complexes: Synthesis and Migratory Insertion Reactions. *Organometallics* **2006**, *25*, 3394–3406. [[CrossRef](#)] [[PubMed](#)]
20. Anderson, L.L.; Arnold, J.; Bergman, R.G. Catalytic Hydroamination of Alkynes and Norbornene with Neutral and Cationic Tantalum Imido Complexes. *Org. Lett.* **2004**, *6*, 2519–2522. [[CrossRef](#)] [[PubMed](#)]
21. Tomson, N.C.; Arnold, J.; Bergman, R.G. Synthesis and Reactivity of Cationic Niobium and Tantalum Methyl Complexes Supported by Imido and  $\beta$ -diketiminato Ligands. *Dalton Trans.* **2011**, *40*, 7718–7729. [[CrossRef](#)] [[PubMed](#)]
22. Stahl, N.G.; Salata, M.R.; Marks, T.J.  $\text{B}(\text{C}_6\text{F}_5)_3$ - vs.  $\text{Al}(\text{C}_6\text{F}_5)_3$ -Derived Metallocenium Ion Pairs. Structural, Thermochemical, and Structural Dynamic Divergences. *J. Am. Chem. Soc.* **2005**, *127*, 10898–10909. [[CrossRef](#)] [[PubMed](#)]
23. Mathis, D.; Couzijn, E.P.A.; Chen, P. Structure, Dynamics, and Polymerization Activity of Zirconocenium Ion Pairs Generated with Boron- $\text{C}_6\text{F}_5$  Compounds and  $\text{Al}_2\text{R}_6$ . *Organometallics* **2011**, *30*, 3834–3843. [[CrossRef](#)]
24. Alonso-Moreno, C.; Lancaster, S.J.; Wright, J.A.; Hughes, D.L.; Zuccaccia, C.; Correa, A.; Macchioni, A.; Cavallo, L.; Bochmann, M. Ligand Mobility and Solution Structures of the Metallocenium Ion Pairs  $[\text{Me}_2\text{C}(\text{Cp})(\text{fluorenyl})\text{MCH}_2\text{SiMe}_3^+\cdots\text{X}^-]$  ( $\text{M} = \text{Zr}, \text{Hf}$ ;  $\text{X} = \text{MeB}(\text{C}_6\text{F}_5)_3, \text{B}(\text{C}_6\text{F}_5)_4$ ). *Organometallics* **2008**, *27*, 5474–5487. [[CrossRef](#)]
25. Spitzmesser, S.K.; Gibson, V.C. Dialkylaluminum Complexes Derived from 1,8-diphenyl-3,6-dimethylcarbazole: a New Sterically Hindered Monodentate Ligand System. *J. Organomet. Chem.* **2003**, *673*, 95–101. [[CrossRef](#)]
26. Gillis, D.J.; Tudoret, M.-J.; Baird, M.C. Novel Arene Complexes of Titanium(IV), Zirconium(IV), and Hafnium(IV). *J. Am. Chem. Soc.* **1993**, *115*, 2543–2545. [[CrossRef](#)]
27. Preparation of  $[\text{TaMe}_4^+ \text{B}(\text{C}_6\text{F}_5)_3\text{Me}^-](2)$ : A cold solution ( $-40^\circ\text{C}$ ) of  $\text{B}(\text{C}_6\text{F}_5)_3$  (125 mg, 0.25 mmol) in dichloromethane was added drop wise to the cold ( $-40^\circ\text{C}$ ) solution of tantalumpentamethyl (50 mg, 0.2 mmol) in dichloromethane. The mixture was stirred for another 15 minutes. Colour of the solution intensified to dark yellowish which indicated the formation of the ionic complex.  $^1\text{H-NMR}$ (600 MHz)  $\delta$  (ppm) 0.5(s, 3H,  $\text{BCH}_3$ ), 2.6(s, 12H,  $\text{TaCH}_3$ ).  $^{13}\text{C-NMR}$ (150 MHz)  $\delta$  (ppm) 10.8(s, 1C,  $\text{BCH}_3$ ), 110.9 (s, 4C,  $\text{TaCH}_3$ ). (Caution! This 8e- compound is highly unstable and decomposes into black tantalum powder while drying.).
28. All the DFT calculations were performed with the Gaussian09, using the PBE0 functional, corrected by the D3 Grimme pairwise scheme, using the SVP basis set except for the metals the standard SDD. Single-point energy calculations in solution (SMD) were performed with the M06 functional and the Def2TZVPP basis set for main group atoms and again the same SDD pseudopotential for the metals.
29. Martin, R.L.; Hay, P.J.; Pratt, L.R. Hydrolysis of Ferric Ion in Water and Conformational Equilibrium. *J. Phys. Chem. A* **1998**, *102*, 3565–3573. [[CrossRef](#)]



30. Poater, A.; Pump, E.; Vummaleti, S.V.C.; Cavallo, L. The Right Computational Recipe for Olefin Metathesis with Ru-Based Catalysts: The Whole Mechanism of Ring-Closing Olefin Metathesis. *J. Chem. Theory Comput.* **2014**, *10*, 4442–4448. [[CrossRef](#)] [[PubMed](#)]
31. Pump, E.; Slugovc, C.; Cavallo, L.; Poater, A. Mechanism of the Ru–allenylidene to Ru–Indenylidene Rearrangement in Ruthenium Precatalysts for Olefin Metathesis. *Organometallics* **2015**, *34*, 3107–3111. [[CrossRef](#)]
32. Manzini, S.; Poater, A.; Nelson, D.J.; Cavallo, L.; Nolan, S.P. How Phenyl Makes a Difference: Mechanistic Insights into the Ruthenium(II)-Catalysed Isomerisation of Allylic Alcohols. *Chem. Sci.* **2014**, *5*, 180–188. [[CrossRef](#)]
33. Manzini, S.; Poater, A.; Nelson, D.J.; Cavallo, L.; Slawin, A.M.Z.; Nolan, S.P. Insights into the Decomposition of Olefin Metathesis Precatalysts. *Angew. Chem. Int. Ed.* **2014**, *53*, 8995–8999. [[CrossRef](#)] [[PubMed](#)]
34. Richmond, C.J.; Matheu, R.; Poater, A.; Falivene, L.; Benet-Buchholz, J.; Sala, X.; Cavallo, L.; Llobet, A. Supramolecular Water Oxidation with Ru-bda-based Catalysts. *Chem. Eur. J.* **2014**, *20*, 17282–17286. [[CrossRef](#)] [[PubMed](#)]
35. Falivene, L.; Credendino, R.; Poater, A.; Petta, A.; Serra, L.; Oliva, R.; Scarano, V.; Cavallo, L. SambVca 2. A Web Tool for Analyzing Catalytic Pockets with Topographic Steric Maps. *Organometallics* **2016**, *35*, 2286–2293. [[CrossRef](#)]
36. Poater, A.; Cosenza, B.; Correa, A.; Giudice, S.; Ragone, F.; Scarano, V.; Cavallo, L. SambVca: A Web Application for the Calculation of Buried Volumes of N-Heterocyclic Carbene Ligands. *Eur. J. Inorg. Chem.* **2009**, *2009*, 1759–1766. [[CrossRef](#)]
37. Poater, A.; Ragone, F.; Giudice, S.; Costabile, C.; Dorta, R.; Nolan, S.P.; Cavallo, L. Thermodynamics of N-Heterocyclic Carbene Dimerization: The Balance of Sterics and Electronics. *Organometallics* **2008**, *27*, 2679–2681. [[CrossRef](#)]
38. Poater, A.; Falivene, L.; Urbina-Blanco, C.A.; Manzini, S.; Nolan, S.P.; Cavallo, L. How does the Addition of Steric Hindrance to a Typical N-Heterocyclic Carbene Ligand Affect Catalytic Activity in Olefin Metathesis? *Dalton Trans.* **2013**, *42*, 7433–7439. [[CrossRef](#)] [[PubMed](#)]



© 2018 by the authors. Licensee MDPI, Basel, Switzerland. This article is an open access article distributed under the terms and conditions of the Creative Commons Attribution (CC BY) license (<http://creativecommons.org/licenses/by/4.0/>).